Mine Water Environ (2016) 35:337–349
DOI 10.1007/s10230-015-0368-y

TECHNICAL ARTICLE

The Effects of Caving of a Coal Mine's Immediate Roof on Floor Strata Failure and Water Inrush

Dongjing Xu[1,2] · Suping Peng[1] · Shiyao Xiang[2] · Mingxing Liang[1,2] · Wenming Liu[3]

Received: 29 March 2015 / Accepted: 5 October 2015 / Published online: 14 October 2015

Abstract Large scale roof strata caving that occurs during coal extraction can irreversibly damage floor strata and result in riskier mining operations. Four research models incorporating floor water pressure were assessed for floor strata failure, using eight methods and two classification systems. A connection between floor strata failure and the coefficient of impact risk was developed. The derived equations represent a potentially effective method for providing a preliminary assessment of the risks associated with floor strata failure due to caving. A classification system of floor failure potential can be constructed to minimize risks during mining.

Keywords Impact loading · Coefficient of impact resistance · Floor water inrush · Plate-beam theory

Electronic supplementary material The online version of this article (doi:10.1007/s10230-015-0368-y) contains supplementary material, which is available to authorized users.

✉ Dongjing Xu
xudongjinggg@126.com

Suping Peng
psp@cumtb.edu.cn

Shiyao Xiang
xiangshiyao1989@163.com

Mingxing Liang
m.liang.cn@gmail.com

Wenming Liu
liuwm0506@126.com

[1] State Key Laboratory of Coal Resource and Safe Mining, China University of Mining and Technology, Beijing 100083, China

[2] College of Geoscience and Surveying Engineering, China University of Mining and Technology, Beijing 100083, China

[3] Xi'an Research Institute Co. Ltd. of China Coal Technology & Engineering Group Corp, Xi'an 710077, China

Introduction

For more than a century, there has been a growing demand for coal resources around the world. Hence, the depth at which coal deposits are extracted has increased considerably (Please et al. 2013; Singh and Singh 2009). Deep coal mining has inherent risks associated with it due to in situ stress and hydraulic damage conditions produced by the overburden pressure, tectonic movements, and pressurized water in aquifers underlying the floor strata (Dong et al. 2012; Li 1999; Peng 2008). Longwall mining is commonly used for underground coal extraction (Abbas et al. 2012; Singh 2014). The removal of the mined panel and the associated overlying roof strata during longwall extraction can be divided into three stages of collapse: the false roof, consisting of thinly bedded and weak rock, usually with intercalated coal bands); the immediate roof, consisting of competent strata above the false roof or directly exposed in the absence of a false roof; and the main roof, above the immediate roof and usually represented by strong strata that do not break or bend until all of the coal is removed (Peng 2008). As the mine panel advances, the immediate roof is supposed to fall, but large-scale roof strata collapse may occur under certain conditions, such as an ultra-thick immediate roof, brittle floor material, etc. (Anon 1995; Mojtaba et al. 2013; Sainoki and Mitri 2014), and these can damage the floor strata. A real-world example is briefly discussed below to illustrate how the impact of this roof rock can increase the likelihood or magnitude of a water inrush event.

By counting and analyzing the location of floor water inrush points from mining areas in northern and eastern China, we know that the distance between the coal wall and water inrush point is typically 0–20 m, and that ≈87 % are within the range of 2–8 m. Additionally, the highest water-inrush rate was 25–35 m from the beginning of the face (Zhang et al. 1992). However, on June 18, 2010, a large-scale roof collapse occurred at the 21,106 working face in the Huafeng coal mine in China when this working face was 46 m from the beginning of the face. This was immediately followed by water inrush through the floor strata at an initial rate of 3 m^3/h, and stabilizing at 20 m^3/h. Although the water emission from this aquifer was not large, it occurred in an area without structural influence, and based on the confluence of events, we believe that the floor water inrush was induced by the impact, and that the impact of a caving roof should not be ignored.

Methods exist to reduce the risks associated with roof control for sustainable, safe, and efficient longwall extraction (Singh and Singh 2009; Singh 2014). Theoretical and empirical models based on the plate-beam theory and bending moment approach (Majumdar 1986; Obert and Duvall 1967) can be used to assess the caving behavior of roof strata. These models can predict main fall (Bilinski and Konopko 1973; Pawlowicz 1967; Peng and Chiang 1984; Singh and Singh 1979, 1982; Unrug and Szwilski 1980) and periodic caving spanning from the immediate or main roof (Kuznetsov et al. 1973; Peng and Chiang 1984; Sarkar and Chatterjee 1992; Sarkar and Dhar 1993; Sarkar et al. 1988). This paper focuses on floor strata failure that results from large-scale roof strata caving, using impact loading mechanics and plate-beam theory (Adler and Sun 1968; Gere and Goodno 2011; Hanna et al. 1991; Obert and Duvall 1967). By understanding caving strata behavior and the uncertainty of its effect on the floor strata, it becomes possible to account for the impact of these factors on the potential of floor water inrush.

Previous Models

Dome Model

The dome model, which is based on Fayol's (1885) laboratory observations (as cited in Tsesarsky and Hatzor 2003), postulated that underground movement is limited by the dome over the area of excavation, with its amplitude diminishing by degrees as it extends farther away from that center. Furthermore, the axis of the dome is presumed to be vertical when coal seams are horizontal (Adler and Sun 1968).

Plate Model

An equation was developed by Obert and Duvall (1967) based on plate theory (Timoshenko and Woinowsky-Krieger 1959) to simulate roof failure during main fall at a longwall panel. This equation computes the maximum tensile stress and deflection for a uniformly gravity-loaded, clamped edge plate (see Supplemental Equation 1; Hanna et al. 1991). The maximum deflection occurs at the center of the plate and is given in Supplemental Equation (2). (Note: supplemental equations and figures accompany the on-line version of this manuscript).

Beam Model

In line with the plate model from Obert and Duvall (1967), when the value of c/a is greater than two, the effect of the lateral dimension can be neglected. Hence, the beam theory can be applied to the plate model (Supplemental Figure 1). Based on the theory of the mechanics of materials, the beam model considers the immediate roof to be a simple beam supported at both ends by pillars (Supplemental Figure 1). Moreover, the load on the beam comes from its own weight and depends on the thickness of the beam, with the downward load force being vertical (Chugh and Missavage 1981; Mueller 2010). Then, the maximum tensile stress can be obtained at both ends of the support (see Supplemental Equation 3) (Beer and Johnston 2005; Gere and Goodno 2011; Manteghi et al. 2012; Singh and Singh 2009, Singh 2014; Tahoony 2009).

Replacing q in Supplemental Equation (4) with Supplemental Equation (7); using Supplemental Equations (4), (5) and (6) for (3) to solve for L_b yields Supplemental Equation (8). In the same way, if the model considers the immediate roof as a fixed beam supported at both ends by the pillars (see Supplemental Figure 2), then the right-hand side of Supplemental Equation (4) turns into $qL_b^2/12$, producing Supplemental Equation (9).

Peng and Chiang (1984) proposed a dimensionally correct method of estimating the span of the main fall (Supplemental Equation 10). Evans (1941) performed a seminal set of investigations of roof deformation mechanics and established the notion of a 'voussoir beam' spanning an excavation, using an analogy with the voussoir arch considered in masonry structures (Brady and Brown 2004). These modes of failure, summarized by Diederichs and Kaiser (1999), are buckling or snap-through failure, lateral compressive failure (crushing) at the midspan and abutments, abutment slip, and diagonal fracturing (DuBois 2009; Sterling 1980).

Models for Predicting Floor Water Inrush

Deep coal mining is at risk when underlain by a high-pressure aquifer system in the floor (Huang et al. 2014; Xu 2010). This has resulted in numerous water inrush events. Thus, the need to take preventive measures cannot be overemphasized. The following models summarize current knowledge regarding water inrush in coal mines.

Relative Aquiclude Thickness

The theory of relative aquiclude thickness first conceptualizes the relationship between underwater pressure, aquiclude thickness, and floor water inrush, taking the lithology and strength of the aquiclude into consideration (Supplemental Equation 11; Wang et al. 1994).

Water Inrush Coefficient

The water inrush coefficient (Supplemental Equation 12) was proposed by the Xi'an Branch of the China Coal Research Institute (CCRI; Jin 2006; Liu 2014; Peng and Chiang 1982; Shi 1985; Shi and Han 2004; Zhao 1985).

Lower Three-Zones

Based on in situ measurements of floor deformation as the mined panel advances, as well as laboratory and numerical simulations, the floor strata can be divided into three main zones: the mine-damaged area, the effective aquiclude, and the confined water-flowing zone. The mine-damaged zone is defined as the strata in which the water transmissibility has obviously changed. Meanwhile, as the consistency of the floor strata is destroyed by the pressure, the effective aquiclude zone represents the portion of the floor strata that retains its integrity, which can prevent the intrusion of water. The confined water-flowing zone refers to the strata damaged by intrusion from the aquifer underlying the floor strata. Hence, the water resistance of the floor strata mainly depends on the effective aquiclude zone, until groundwater intrusion cannot be prevented any longer (Li et al. 1988; Li 1999; Liu 2014; Shen et al. 1992).

Impact Study Models

Few inrush models incorporate the induced effects of caving of the immediate roof. These effects may be investigated using two collapsing models (Hu and Yin 2010). Using impact loading in the mechanics of materials (Beer and Johnston 2005), we can assume that the caving of the immediate roof would produce dynamic effects on the floor strata when its length reaches the failure span of the immediate roof as a beam model; thereafter, we can use Supplemental Equation (8) from Obert and Duvall (1967) and Supplemental Equation (9) as the caving length of the immediate roof. Assuming that the immediate roof ideally collapses, either one, large intact mass drops, or the roof breaks at the middle of the beam, with the immediate roof divided in half (Supplemental Figures 3 and 4, respectively).

To perform a simplified analysis of this complex situation, the caving behavior is idealized to the immediate roof striking the floor strata, which is analogous to that of the impact of an object falling onto the floor beam. Further assuming that the strata between the coal seam and the underlying aquifer can be viewed as a simple beam supported at both ends suggests that burst pressure and karstification may cause the aquifer to fail and create space for the water to move (Brady and Brown 2004; Gere and Goodno 2011; Hu and Yin 2010; Zhou et al. 2014). Because the caving and the impact of the immediate roof is a complex process mixed with a series of mechanical changes and controlled by a variety of factors, we only discuss the effects of the instant impact state without considering that of cyclical loading and floor heaving due to unloading. A detailed qualitative analysis on the effects of these unconsidered factors can be found in the results and discussion section.

It is well known that the geological composition of the floor material determines not only the water-resistant ability of floor strata (Bai et al. 2009; Zhang 2014; Zhu et al. 2014), but also whether the floor has dynamic deflection potential. Engineering practices have shown that mine floors often contain clay, mudstone, and siltstone. In this article, we only consider the floor strata as hard rock that has dynamic deflection potential to apply the beam theory for a better and more targeted analysis on the impact of caving. Additionally, we consider the failure zone of the aquifer as a prerequisite for building the floor beam model; this factor and its relationship to water inrush will be considered and analyzed in a later section.

Using the principle of conservation of energy, by equating the potential energy lost by the falling mass to the maximum strain energy acquired by the floor beam, and applying the impact factor of the mechanics of materials into the research on those impact models (Gere and Goodno 2011), we obtain:

$$\text{Impact factor} = \frac{\delta_{dy}}{\delta_{st}} = \left[1 + \left(1 + \frac{2h_{dy}}{\delta_{st}}\right)^{1/2}\right] \quad (1)$$

where δ_{dy} is the maximum dynamic deflection of the beam (m), δ_{st} is the static deflection of the beam (m); and h_{dy} is the falling height of the caving roof corresponding to the

floor beam (m). Then, we obtain the following equation for the maximum dynamic tensile stress:

$$\sigma_{dy} = \sigma_{st}\left[1 + \left(1 + \frac{2h_{dy}}{\delta_{st}}\right)^{1/2}\right] \tag{2}$$

where σ_{dy} is the maximum dynamic tensile stress (MPa) and σ_{st} is the stress when the load acts statically (MPa). What the models infer in this article is point focused, and the center of gravity from the caving roof is taken as a focused point. As long as the falling height h_{dy} is significantly larger than the static deflection δ_{st} of the coal mining, we can simplify Eq. (2) to:

$$\sigma_{dy} = \sigma_{st}\left(\frac{2h_{dy}}{\delta_{st}}\right)^{1/2} \tag{3}$$

Model Study I

In this section, we introduce the simple supported beam model of the immediate roof subject to uniform loading. The impact model of the immediate roof in the first type of caving form can further fall into two cases, depending on the mechanical behavior of the water pressure from the underlying aquifer.

Disregarding Underwater Pressure

This model is expressed in Fig. 1. In addition, the maximum tensile stress of the floor beam, σ_b (MPa), is given by:

$$\sigma_b = \frac{M_b C_b}{I_b} \tag{4}$$

where:

$$M_b = \frac{q_b L_b^2}{8} \tag{5}$$

$$C_b = \frac{h'}{2} \tag{6}$$

$$I_b = \frac{bh'^3}{12} \tag{7}$$

where L_b is given in Supplemental Equation (8), C_b is the neutral axis distance of the floor beam from the neutral surface (m), I_b is the moment of inertia (m^4), M_b is the maximum bending moment (N·m), h' is the thickness of the floor beam (m), q_b is the uniform load of the unit area, and the value of q_b is $\gamma bh'$. Substituting the right-hand side of Eq. (4) with Eqs. (5), (6), and (7), and solving for σ_b, we obtain the following equation:

$$\sigma_b = \frac{3\gamma L_b^2}{4h'} = \frac{3h\sigma_t}{2h'} \tag{8}$$

Similarly, we can obtain the stress if the mechanical behavior of the caving roof acts on the floor beam statically:

$$\sigma_{st} = \frac{M_{st} C_b}{I_b} \tag{9}$$

Meanwhile, we obtain

$$M_{st} = \frac{q_{st} L_b^2}{8} \tag{10}$$

$$C_b = \frac{h'}{2} \tag{11}$$

$$I_b = \frac{bh'^3}{12} \tag{12}$$

where M_{st} is the maximum bending moment when acting statically (N·m); q_{st} is the uniform load of the unit area, and the value of q_{st} is γbh. Substituting the right-hand side of

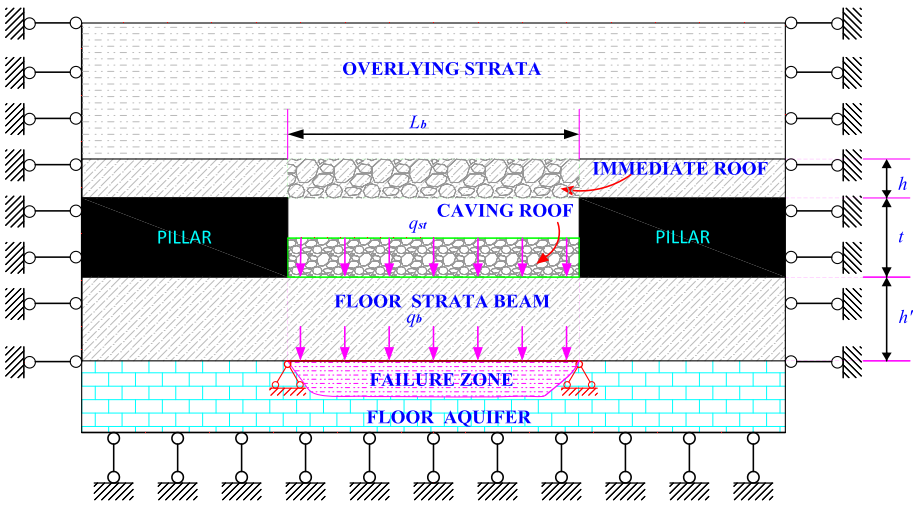

Fig. 1 Schematic diagram illustrating the dynamic impact model of the immediate roof disregarding underwater pressures in the first caving form

Eq. (9) with Eqs. (10), (11), and (12), and solving for σ_{st}, we obtain the following equation:

$$\sigma_{st} = \frac{3\gamma h L_b^2}{4h'^2} = \frac{3h^2\sigma_t}{2h'^2} \tag{13}$$

Furthermore, we can obtain the static deflection of the simple beam supported at both ends subjected to the uniform loading of q_{st}:

$$\delta_{st} = \frac{5q_{st}L_b^4}{384EI_b} = \frac{5\gamma h L_b^4}{32Eh'^3} = \frac{5h^3\sigma_t^2}{8\gamma Eh'^3} \tag{14}$$

With this caving type of the immediate roof, the falling height h_{dy} equals the thickness of the coal seam t (m). Thus, substituting the right-hand side of Eq. (3) with Eqs. (13) and (14) yields:

$$\sigma_{dy} = \frac{6\sqrt{5}}{5}\sqrt{t\gamma E}\cdot\sqrt{\frac{h}{h'}} \tag{15}$$

According to the method of the superposition of the mechanics of materials, only when the value of σ_{dy} plus σ_b surpasses the tensile strength of the floor strata, σ_t, does the floor beam break and floor water inrush occur, producing:

$$\sigma_{dy} + \sigma_b = \sigma_t \tag{16}$$

Then, by using Eq. (8) and (15), Eq. (16) for assessing the failure of the floor beam and floor water inrush becomes:

$$\frac{3h\sigma_t}{2h'} + \frac{6\sqrt{5}}{5}\sqrt{t\gamma E}\cdot\sqrt{\frac{h}{h'}} - \sigma_t = 0 \tag{17}$$

This equation is quadratic and can be solved for the positive root, with the following result:

$$\sqrt{\frac{h}{h'}} = \frac{\sqrt{\frac{4t\gamma E}{5} + \frac{2\sigma_t^2}{3}} - \frac{2\sqrt{5}}{5}\sqrt{t\gamma E}}{\sigma_t} \tag{18}$$

Exchanging the position of h and h' in Eq. (18), we obtain the ratio of the thickness of the floor beam to the thickness of the immediate roof, which may show the ability of the floor beam to resist the impact caused by caving of the immediate roof. This equation reveals that different thicknesses between the floor beam and the immediate roof would have different effects on the floor failure. Generally speaking, the thicker the floor beam and the thinner the caving roof, the smaller the impact effect will be on the floor and the safer coal mining becomes. Therefore, this ratio can be defined as the coefficient of impact risk (CIR), which is given in Eq. (19).

$$\mathrm{CIR} = \frac{h'}{h} \tag{19}$$

where h' is the thickness of the floor beam (m), h is the thickness of the immediate roof (m), and CIR is dimensionless. This equation conceptualizes the relationship between the thickness of the floor beam, the thickness of the immediate roof, floor failure, and water inrush, taking impact loading and the beam theory into consideration. Meanwhile, it shows the risk degrees of the effect of an impact on the floor. When this coefficient exceeds a certain critical value, floor failure will occur at both ends of the floor beam where the tensile stress is maximized; cracks will develop in that position, causing water inrush. Then, Eq. (18) becomes:

$$\mathrm{CIR} = \frac{h'}{h} = \left[\frac{\sigma_t}{\sqrt{\frac{4t\gamma E}{5} + \frac{2\sigma_t^2}{3}} - \frac{2\sqrt{5}}{5}\sqrt{t\gamma E}}\right]^2 \tag{20}$$

Based on Eq. (20), we know that the right-hand side of the equation is the critical value that can be obtained using the values of t, γ, E, and σ_t obtained from actual exploration. If the value of CIR is less than the critical value, the floor beam cannot bear the impact of a caving roof. Meanwhile, stress failure at both ends of the floor beam may occur, and floor water inrush would occur along both sides of the crack. In this model, the effect of underwater pressure is not considered, and only the floor failure induced by caving is considered to cause the water inrush. At the Huafeng coal mine example cited earlier, the mining height of the working face was 2.2 m, and the thickness of the immediate roof was up to 4 m, with a lithology of siltstone, which is a roof type that resists caving. Its floor strata was a slightly hard marl, which was only 26 m above a limestone aquifer. Thus, the mine had a CIR value of 6.5. This illustrates how CIR can be used to predict floor failure and water inrush. By weighing the magnitude between the CIR and the critical value in advance, we can understand the degree of risk posed by such an impact, and whether this might be a factor to consider with respect to floor water inrush.

Taking the Underwater Pressure into Account

Due to the effect of the underwater pressure on the floor beam, we know the value of q_b from Eq. (5) will change from γbh to $(\gamma bh - P_w b)$, in which P_w is the groundwater pressure from the aquifer underlying the floor strata. This model is shown in Fig. 2. In a similar manner, Eq. (16) now becomes:

$$\frac{6\sqrt{5}}{5}\sqrt{t\gamma E}\cdot\sqrt{\frac{h}{h'}} + \frac{3h\sigma_t(\gamma h' - P_w)}{2\gamma h'^2} = \sigma_t \tag{21}$$

Solving Eq. (21) for P_w, yields:

$$P_w = \gamma h'\left(\frac{4\sqrt{5}}{5\sigma_t}\sqrt{t\gamma E}\cdot\sqrt{\frac{h'}{h}} - \frac{2h'}{3h} + 1\right) \tag{22}$$

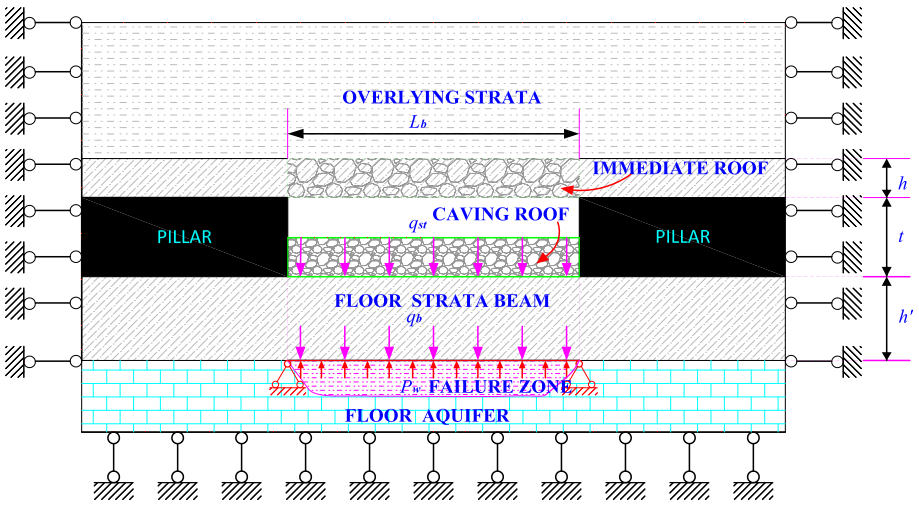

Fig. 2 Schematic diagram illustrating the dynamic impact model of the immediate roof taking underwater pressures into account in the first caving form

In this model, the underwater pressure, and its effect on the instant impact of a caving roof are also considered. In this case, underwater pressure plays a role in resisting the impact of a caving roof. Equation (22) is obtained by the application of impact loading and the beam theory, and the right-hand side of the equation is the critical value that can be obtained by using the values of t, γ, E, σ_t, h' and h obtained from actual exploration. Generally speaking, when the value of P_w is lower than the critical value at the moment of impact, the floor beam cannot bear the impact of the caving roof. Meanwhile, stress failure at both ends of the floor beam may occur, and floor water inrush would occur along both sides of the crack.

Model Study II

As discussed above, the other type of caving roof breaks at the midpoint of the beam, with the immediate roof divided in half, as shown in Supplemental Figure 4, with both points B and B' representing the cracked midpoints. For a better analysis, we make several appropriate simplifications:

- When the immediate roof collapses, it will produce two key acting forces F_1 and F_2, having points C_1 and C_2, respectively, on the contact surface with the floor strata, as shown in Fig. 3.
- The mechanical effect of the overlying strata on the immediate roof is ignored, as are the friction force and the holding power from both ends in the process of caving. Thus, we can use the value of gravitational force, G_1 and G_2, of the two roof sections as F_1 and F_2, respectively. We obtain:

$$F_1 = F_2 = \frac{\gamma b h L_b}{2} \tag{23}$$

Then, we can treat the strata between the coal seam and the underlying aquifer as a simple supported beam subjected to two concentrated loads that have the same distance from both ends. As shown in Fig. 3, points O_1 and point O_2 are the centers of gravity of the two parts, and points O_1' and O_2' are the same points after the immediate roof collapses and strikes the floor. Thus, the height of O_1O_1' or O_2O_2' is the falling height of the caving roof, named $L_{O1O1'}$ or $L_{O2O2'}$,respectively. According to the sum of the interior angles of a triangle and $\angle A_1C_1B' = 90°$, we know that $\angle A_1C_1D_1 = \angle C_1B'B'' = \alpha$. Meanwhile, the sine and cosine law of a right-angled triangle can be used to obtain:

$$\sin\alpha = \frac{L_{C_1B''}}{L_{C_1B'}} = \frac{L_{A_1D_1}}{L_{A_1C_1}} \tag{24}$$

$$\cos\alpha = \frac{L_{B'B''}}{L_{C_1B'}} = \frac{L_{D_1C_1}}{L_{A_1C_1}} \tag{25}$$

where the length of C_1B'' and D_1C_1 can be separately expressed by $L_{C1B''}$ and L_{D1C1}, respectively; the same as that of A_1C_1, A_1D_1, C_1B', BB', and $B'B''$, and the value of $L_{C1B''}$ plus L_{D1C1} equals that of L_{A1C1}. In addition, the values of $L_{C1B'}$ and L_{A1D1} are h and t, respectively. Therefore, Eqs. (24) and (25) become:

$$\sin\alpha = \frac{L_{C_1B''}}{h} = \frac{t}{L_b/2} \tag{26}$$

$$\cos\alpha = \frac{L_{B'B''}}{h} = \frac{L_{D_1C_1}}{L_b/2} \tag{27}$$

Solving Eq. (26) for $L_{C1B''}$ yields:

$$L_{C_1B''} = \frac{2th}{L_b} \tag{28}$$

Because B'' is the midpoint of D_1C_2, we obtain:

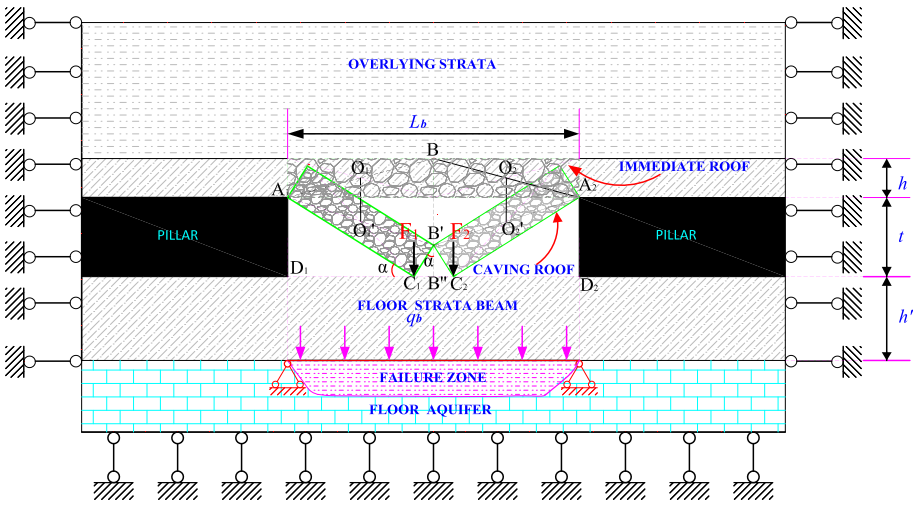

Fig. 3 Schematic diagram illustrating the dynamic impact model of the immediate roof disregarding underwater pressures in the second caving form

$$L_{C_1B''} + L_{D_1C_1} = \frac{L_b}{2} \tag{29}$$

Substituting Eq. (29) for Eq. (28) and solving for L_{D1C1}:

$$L_{D_1C_1} = \frac{L_b^2 - 4th}{2L_b} \tag{30}$$

In addition, due to Pythagoras' Theorem, we obtain the following equation from $\Delta A_1D_1C_1$, yielding:

$$L_{D_1C_1}^2 = L_{A_1C_1}^2 - L_{A_1D_1}^2 = \frac{L_b^2}{4} - t^2 = \frac{L_b^2 - 4t^2}{4} \tag{31}$$

Substituting Eq. (27) for Eq. (30) and solving for $L_{B'B''}$ yields:

$$L_{B'B''} = \frac{h(L_b^2 - 4th)}{L_b^2} \tag{32}$$

Meanwhile,

$$L_{BB'} + L_{B'B''} = t + h \tag{33}$$

Substituting Eq. (33) by Eq. (32) and solving for $L_{BB'}$:

$$L_{BB'} = \frac{t(L_b^2 + 4h^2)}{L_b^2} \tag{34}$$

Applying the law of a median of a triangle to $\Delta A_1BB'$, we can obtain the falling height of the caving roof in the light of impact model:

$$h_{dy} = L_{O_1O_1'} = L_{O_2O_2'} = \frac{L_{BB'}}{2} = \frac{t(L_b^2 + 4h^2)}{2L_b^2} \tag{35}$$

Based on a simple supported beam subjected to two concentrated loads that have the same distance from both ends, we know that:

$$M_{st} = F_1 L_{D_1C_1} \tag{36}$$

$$\delta_{st} = \frac{F_1 L_{D_1C_1}(3L_b^2 - 4L_{D_1C_1}^2)}{24EI_b} \tag{37}$$

Substituting the right-hand side of Eq. (9) with Eqs. (11), (12), (23), and (36) and solving for σ_{st}, we obtain:

$$\sigma_{st} = \frac{3\gamma h(L_b^2 - 4th)}{2h'^2} \tag{38}$$

Moreover, substituting the right-hand side of Eq. (36) with Eqs. (12), (23), and (30) and solving for δ_{st}, we obtain:

$$\delta_{st} = \frac{\gamma h(L_b^2 - 4th)(L_b^2 + 2t^2)}{4Eh'^3} \tag{39}$$

Thus, substituting the right-hand side of Eq. (3) with Eqs. (35), (38), and (39) yields:

$$\sigma_{dy} = 3\sqrt{\frac{t\gamma Eh(L_b^2 + 4h^2)(L_b^2 - 4th)}{h'L_b^2(L_b^2 + 2t^2)}} \tag{40}$$

Furthermore, the impact model of the immediate roof in this type of caving can also be divided into two cases, similar to the first type.

Disregarding Underwater Pressure

As shown in Fig. 3, in this model, the maximum tensile stress of the floor beam itself, σ_b (MPa), still adopts the means of expression given in Eq. (8), and the maximum dynamic tensile stress, σ_{dy} (MPa), adopts the form of Eq. (40). Then, replacing L_b by Supplemental Equation (8) before substituting Eq. (16) all together, we can calculate and create an appropriate form, as follows:

$$\frac{h'}{h} + \frac{9h}{4h'} = 3 + \frac{9t\gamma Eh(\sigma_t + 2\gamma h)(\sigma_t - 2t\gamma)}{\sigma_t^3(h\sigma_t + t^2\gamma)} \tag{41}$$

Incorporating CIR into Eq. (41) yields:

$$\mathrm{CIR}+\frac{9}{4\mathrm{CIR}}=3+\frac{9t\gamma Eh(\sigma_t+2\gamma h)(\sigma_t-2t\gamma)}{\sigma_t^3(h\sigma_t+t^2\gamma)} \tag{42}$$

From this equation, we know that the right-hand side of Eq. (42) is the critical value that can be obtained by using the values of t, γ, E, σ_t, and h obtained from actual exploration. If the left-hand side is less than the critical value, the floor beam cannot bear the impact of caving roof, stress failure may happen at both ends of floor beam, and floor water inrush would occur along both sides of the crack.

Taking Underwater Pressure into Account

As shown in Fig. 4, in this model, the value of q_b from Eq. (5) changes from $\gamma bh'$ to $(\gamma bh - P_w b)$, as in the second situation in model study *I*. Then, the maximum tensile stress of the floor beam, σ_b (MPa), becomes:

$$\sigma_b=\frac{3L_b^2(\gamma h'-P_w)}{4h'^2}=\frac{3h\sigma_t(\gamma h'-P_w)}{2\gamma h'^2} \tag{43}$$

Substituting Eq. (16) into Eqs. (40) and (43) and solving for P_w, we obtain:

$$P_w=\gamma h'\left(2\sqrt{\frac{t\gamma Eh'(\sigma_t+2\gamma h)(\sigma_t-2t\gamma)}{\sigma_t^3(h\sigma_t+t^2\gamma)}}-\frac{2h'}{3h}+1\right) \tag{44}$$

As in model study *I*, Eq. (44) is obtained by the application of impact loading and the beam theory, and the right-hand side of the equation is the critical value that can be obtained using the values of t, γ, E, σ_t, h', and h obtained from actual exploration. Generally speaking, when the value of P_w is lower than the critical value at the moment of impact, the floor beam cannot bear the impact of the caving roof. Meanwhile, stress failure at both ends of the floor beam may occur, and floor water inrush would occur along both sides of the crack.

If the caving model of the immediate roof is taken as a fixed beam model subjected to a uniform loading, as shown in Supplemental Figure 2, we can substitute L_b of model studies *I* and *II* from Supplemental Equation (9) and turn them into model studies *III* and *IV*, respectively.

Model Study III

Disregarding Underwater Pressure

Similar to the derivation process of model study *I* and not considering the behavior of underwater pressure, further applying Supplemental Equation (9) to replace L_b of all equations of model study *I*, we obtain:

$$\sigma_b=\frac{h\sigma_t}{h'} \tag{45}$$

$$\sigma_{dy}=\frac{6\sqrt{5}}{5}\sqrt{t\gamma E}\cdot\sqrt{\frac{h}{h'}} \tag{46}$$

Thus, Eq. (16) for assessing the failure of the floor beam and floor water inrush and using Eqs. (45) and (46) becomes:

$$\frac{h\sigma_t}{h'}+\frac{6\sqrt{5}}{5}\sqrt{t\gamma E}\cdot\sqrt{\frac{h}{h'}}-\sigma_t=0 \tag{47}$$

This equation is quadratic and can be solved for the positive root, with the following result:

$$\sqrt{\frac{h}{h'}}=\frac{\sqrt{\frac{9t\gamma E}{5}+\sigma_t^2}-\frac{6\sqrt{5}}{5}\sqrt{t\gamma E}}{\sigma_t} \tag{48}$$

By means of the expression of the CIR, Eq. (48) changes to:

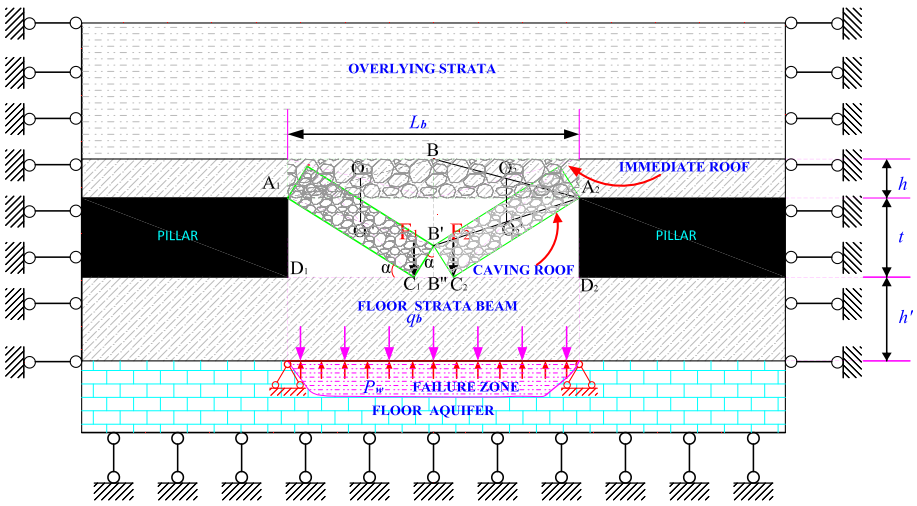

Fig. 4 Schematic diagram illustrating the dynamic impact model of the immediate roof taking underwater pressures into account in the second caving form

$$\mathrm{CIR} = \frac{h'}{h} = \left[\frac{\sigma_t}{\sqrt{\frac{9t\gamma E}{5} + \sigma_t^2} - \frac{6\sqrt{5}}{5}\sqrt{t\gamma E}}\right]^2 \tag{49}$$

From Eq. (49), we know that the right-hand side of the equation is the critical value that can be obtained by using the values of t, γ, E, and σ_t obtained from actual exploration. If the value of the CIR is less than the critical value, the floor beam cannot bear the impact of the caving roof. Meanwhile, stress failure at both ends of the floor beam may occur, and floor water inrush would occur along both sides of the crack.

Taking Underwater Pressure into Account

If the underwater pressure is considered, and again applying Supplemental Equation (9) to replace L_b of all equations of model study *I*, we obtain:

$$\sigma_b = \frac{h\sigma_t(\gamma h' - P_w)}{\gamma h'^2} \tag{50}$$

$$\sigma_{dy} = \frac{6\sqrt{5}}{5}\sqrt{t\gamma E}\cdot\sqrt{\frac{h}{h'}} \tag{51}$$

Then, by using Eqs. (50) and (51), Eq. (16) for assessing the failure of the floor beam and floor water inrush becomes:

$$\frac{h\sigma_t(\gamma h' - P_w)}{\gamma h'^2} + \frac{6\sqrt{5}}{5}\sqrt{t\gamma E}\cdot\sqrt{\frac{h}{h'}} - \sigma_t = 0 \tag{52}$$

Solving for P_w, we obtain:

$$P_w = \gamma h'\left(\frac{6\sqrt{5}}{5\sigma_t}\sqrt{t\gamma E}\cdot\sqrt{\frac{h'}{h}} - \frac{h'}{h} + 1\right) \tag{53}$$

Equation (53) is obtained by the application of impact loading and the beam theory, and the right-hand side of the equation is the critical value that can be obtained by using the values of t, γ, E, σ_t, h' and h obtained from actual exploration. Generally speaking, when the value of P_w is lower than the critical value at the moment of impact, the floor beam cannot bear the impact of the caving roof. Meanwhile, stress failure at both ends of the floor beam may occur, and floor water inrush would occur along both sides of the crack.

Model Study IV

Disregarding Underwater Pressure

Similar to the derivation process of model study *II* and disregarding underwater pressure, further applying Supplemental Equation (9) to replace L_b in all equations of model study *II*, we obtain:

$$\sigma_b = \frac{h\sigma_t}{h'} \tag{54}$$

$$\sigma_{dy} = h\sqrt{\frac{18t\gamma E(\sigma_t + 3\gamma h)(\sigma_t - 3t\gamma)}{h'\sigma_t(2h\sigma_t + 3t^2\gamma)}} \tag{55}$$

Then, by using Eqs. (54) and (55), Eq. (16) for assessing the failure of the floor beam and floor water inrush becomes:

$$\frac{h\sigma_t}{h'} + h\sqrt{\frac{18t\gamma E(\sigma_t + 3\gamma h)(\sigma_t - 3t\gamma)}{h'\sigma_t(2h\sigma_t + 3t^2\gamma)}} - \sigma_t = 0 \tag{56}$$

We further make an appropriate transformation of the form as follows:

$$\frac{h'}{h} + \frac{h}{h'} = 2 + \frac{18t\gamma Eh(\sigma_t + 3\gamma h)(\sigma_t - 3t\gamma)}{\sigma_t^3(2h\sigma_t + 3t^2\gamma)} \tag{57}$$

Applying the CIR to Eq. (57) produces:

$$\mathrm{CIR} + \frac{1}{\mathrm{CIR}} = 2 + \frac{18t\gamma Eh(\sigma_t + 3\gamma h)(\sigma_t - 3t\gamma)}{\sigma_t^3(2h\sigma_t + 3t^2\gamma)} \tag{58}$$

This equation shows that the right-hand side of Eq. (58) is the critical value that could be obtained using the values of t, γ, E, σ_t, and h obtained from actual exploration. If the left-hand side is less than the critical value, the floor beam cannot bear the impact of the caving roof. Meanwhile, stress failure at both ends of the floor beam may occur and floor water inrush would occur along both sides of the crack.

Taking the Underwater Pressure into Account

If the underwater pressure is considered, and again applying Supplemental Equation (9) to replace L_b of all equations of model study *I*, we obtain:

$$\sigma_b = \frac{h\sigma_t(\gamma h' - P_w)}{\gamma h'^2} \tag{59}$$

$$\sigma_{dy} = h\sqrt{\frac{18t\gamma E(\sigma_t + 3\gamma h)(\sigma_t - 3t\gamma)}{h'\sigma_t(2h\sigma_t + 3t^2\gamma)}} \tag{60}$$

Then, by using Eqs. (59) and (60), Eq. (16) for assessing the failure of the floor beam and floor water inrush becomes:

$$\frac{h\sigma_t(\gamma h' - P_w)}{\gamma h'^2} + h\sqrt{\frac{18t\gamma E(\sigma_t + 3\gamma h)(\sigma_t - 3t\gamma)}{h'\sigma_t(2h\sigma_t + 3t^2\gamma)}} - \sigma_t = 0 \tag{61}$$

Solving for P_w, we obtain:

$$P_w = \gamma h'\left(\sqrt{\frac{18t\gamma Eh'(\sigma_t + 3\gamma h)(\sigma_t - 3t\gamma)}{\sigma_t^3(2h\sigma_t + 3t^2\gamma)}} - \frac{h'}{h} + 1\right) \tag{62}$$

Equation (62) is obtained by the application of impact loading and the beam theory, and the right-hand side of the equation is the critical value that can be obtained by using the values of t, γ, E, σ_t, h' and h obtained from actual exploration. Generally speaking, when the value of P_w is less than the critical value at the moment of impact, the floor beam cannot bear the impact of the caving roof, stress failure may occur at both ends of the floor beam, and floor water inrush will occur along both sides of the crack.

Results and Discussion

Impact Effect on Floor Failure and Water Inrush

In this study, these models, which cover two types of beam models of the immediate roof (Supplemental Figures 1 and 2), two types of caving forms of the immediate roof (Supplemental Figures 3 and 4), and two cases that consider the effect of water pressure from the underlying aquifer or not (Figs. 1, 2, 3, 4), are assumed to reveal the instant impact effects of the caving of the immediate roof on the water-resistant floor strata. These models enable us to concentrate solely on the impact failure problem.

The four models above, and model studies *I*, *II*, *III*, and *IV*, produce eight related formula, given as Eqs. (20), (22), (42), (44), (49), (53), (58), and (62). By analyzing the derived formulae, we can determine that there is a close connection between water-resistant floor strata and the CIR.

Equations (20), (49), (42) and (58) clearly show the meaning and practical value of the CIR, which will be very useful in determining the level of impact that water-resistant floor strata can bear. That is, they allow an operator to make full use of the value of parameters such as h, h', t, γ, E, and σ_t obtained from actual exploration and compare the two sides of the equation to predict potential danger. When the value of the left-hand side is larger than the right-hand one, floor water inrush will not occur. Then, accumulating sequentially, we can divide the danger levels of floor strata failure into three categories, as shown in Table 1. For example, before a working panel is selected for extraction, these four equations would be calculated successively. If there is only one that satisfies the condition of causing water inrush, it may be presumed that the floor failure potential and the possibility of water inrush are low and, thus, we do not need to worry about this case. If there are two or three that satisfy the condition of causing water inrush, it may be presumed that the floor failure potential and the possibility of water inrush are medium and that some necessary precautions should be taken. If there are four that satisfy the condition of causing water inrush, it may be presumed that the floor failure potential and the possibility of water inrush are very high and, thus, whether this area should be mined should then be determined using other assessment systems.

Table 1 Danger degree classification of floor strata failure

Degree of danger	Satisfied formula number
High	4
Medium	2–3
Low	1

Because different caving forms of the immediate roof will produce different results, we can roughly assess the danger levels to ensure adequate security of coal mining in a comprehensive manner by considering the equations of the four cases using the acquired geological parameters. Simultaneously, the maximum tensional stress occurs at both ends of the floor beam during the process of impact, causing fracture development on both sides and further allowing water inrush. However, in this study, we only take it as an inducement of floor water inrush, since water inrush is affected by a number of factors such as geological structure, mining pressure, water abundance in the floor aquifer, water pressure, and water-resistant strata. Because in actual engineering practice, water inrush will occur on the floor at points and not in whole sections, we need to perform further analysis on the model results. Although floor failure occurred at both ends of the floor beam, stress failure is also controlled by many factors such as floor heaving and the geological composition of the floor material, which will be discussed below. Additionally, the development of fractures and the influence of water would make the water flow towards the best water channel. This channel may involve some points and not whole fracture sections.

In addition, in this study, we were particularly concerned about floor failure under the instant impact of caving without considering the process of cyclical loading. In addition, floor heaving due to unloading is an important factor for floor failure; it would inevitably withstand an impact in the opposite direction and weaken the effect of that impact. However, considering that this research mainly was focused on the instant state of caving impact, we can ignore the effects of floor heaving at present. During actual production, the geological composition of the floor material also affects its impact resistance capability. Furthermore, the more brittle the floor material (e.g. sandstone and siltstone), the stronger its impact resistance and the less prone to failure the floor strata. Therefore, additional research should be performed regarding this issue.

Influence of Water Pressure

Many different viewpoints have been proposed for the description of floor-confined water. However, most show that floor-confined water reduces rock strength. In this process, water pressure has to overcome the stress of the surrounding strata so that the rock fractures, causing water inrush accidents. In addition, factors such as roof weight, blasting vibrations, and shock bumps could lead to vibration of the groundwater, washing cracks and accelerating their expansion (Wasantha and Ranjith 2014; Xiao 2013; Xu 2010).

Nevertheless, this study reveals a new role for the floor aquifer in weakening the immediate initial impact of the roof and inhibiting the water-resistant part of the floor strata from breaking, as shown in Eqs. (22), (44), (53), and (62). These four equations are derived from those cases corresponding to those of Eqs. (20), (42), (49), and (58), respectively, which only differ by taking water pressure into account. Those equations show the relationship between Pw and some other parameters, including h, h′, t, γ, E, and σ_t. Only if at the moment that the caving roof strikes the water-resistant floor strata with a water pressure less than the right-hand side of the above equations will a floor water inrush accident occur. Similarly, we can also divide the danger levels of floor strata failure considering the floor water pressure into three categories (Table 2). Its detailed assessment is similar to the danger degree classification of floor strata failure.

We propose a comprehensive classification degree of the danger of floor water-rush by combining two cases between Tables 1 and 2. When all eight equations are calculated successively, we can satisfy the condition shown in Table 3. Then, the potential of floor water inrush can be classified by considering the above two cases.

Overall, we can conclude that a floor aquifer would act as a "cushion" and have a comprehensive effect on floor water-resistant strata. At the beginning, mining the coal seam could cause the floor water to vibrate, accelerating floor damage, playing a negative role. Then, the floor water could weaken and resist the rock impact, playing a positive role when the roof collapses. Furthermore, the floor water will again harm the floor strata as the mine panel advances. There could be a trend to change from destroying to weakening and then again destroying, resulting in a circular process. This changing role of the floor aquifer should not be underestimated in the prevention of water inrush accidents and requires further study.

Table 2 Danger degree classification of floor strata failure considering floor water pressure

Degree of danger	Satisfied formula number
High	4
Medium	2–3
Low	1

Table 3 Comprehensive classification degree of danger at floor water-rush

Comprehensive degree of danger	Satisfied formula number
High	7–8
Medium	4–6
Low	2–3

Conclusions

In the course of coal mining, large-scale roof strata caving would have a non-ignorable impact effect on water-resistant floor strata. In this paper, a plate-beam theory model of the roof and floor strata, based on the impact loading of the mechanics of materials, is proposed, which includes eight induced equations for emphasizing the impact failure effect while taking floor water pressure into account. By defining the coefficient of impact resistance (CIR), we can connect the floor failure potential with the CIR more precisely. Although these eight equations are only based on limited parameters, such as h, h', t, γ, E, and σ_t obtained from actual exploration, this model could be used to preliminarily assess the potential dangers of floor strata failure from the impact of a caving roof to prevent floor water inrush at both ends of the floor beam. For floor-confined water, the authors proposed a new idea that its effects increase, then decrease (through cushioning), and then increases the susceptibility of the mine floor to such impacts. Additionally, this trend comes full circle through the whole process of coal mining. The floor failure and water inrush models could provide references for safe mining. However, this subject should be further studied using the theory of the "lower three-zones", which categorizes the floor strata into three main zones. Furthermore, factors such as floor heaving and the geological composition of the floor material also need to be carefully considered in future research.

Acknowledgments Our deepest gratitude goes to the editors and the anonymous reviewers for their careful work and thoughtful suggestions that have helped improve this paper substantially. The authors also gratefully acknowledge the financial support of the National Science and Technology Supporting Program (Grant 2012BAB13B01), National Key Scientific Instrument and Equipment Development Program (Grant 2012YQ030126), Coal United Project

of National Natural Science Foundation (Grant U1261203), China Geological Survey Project (Grant 1212011220798), and the National Science and Technology Major Project (Grant 2011ZX05035-004-001HZ).

References

Abbas M, Ferri PH, Mehdi YN (2012) Prediction of the height of destressed zone above the mined panel roof in longwall coal mining. Int J Coal Geol 98:62–72. doi:10.1016/j.coal.2012.04.005

Adler L, Sun MC (1968) Ground control in bedded formations bull 28. Virginia Polytechnic Institute, Blacksburg

Anon (1995) Longwall mining, office of coal, nuclear, electric and alternate fuels. US Department of Energy, Washington, pp 9–10

Bai XQ, Bai HB, Shen ZH (2009) Relative strata impermeability in Ordovician top and risk assessment of water inrush from coal floor in Xinyi coalfield. Chin J Rock Mech Eng 28(2):273–280

Beer FP, Johnston ER (2005) Mechanics of materials, 4th edn. McGraw Hill, New York City

Bilinski A, Konopko W (1973) Criteria for choice and use of powered supports. In: Proceedings of symposium on protection against roof falls, Katowice, Poland, No. IV-1

Brady BHG, Brown ET (2004) Rock mechanics for underground mining, 3rd edn. Chapman & Hall, London

Chugh YP, Missavage RA (1981) Effects of moisture on strata control in coal mines. Eng Geol 17(4):241–255

Diederichs MS, Kaiser PK (1999) Tensile strength and abutment relaxation as failure control mechanisms in underground excavations. Int J Rock Mech Min Sci 36(1):69–96. doi:10.1016/S0148-9062(98)00179-X

Dong DL, Sun WJ, Xi S (2012) Water-inrush assessment using a GIS-based Bayesian network for the 12-2 coal seam of the Kailuan Donghuantuo coal mine in China. Mine Water Environ 31(2):138–146

Du Bois C (2009) Comprehensive design methodology for coal mining under competent sandstone roof. MS Thesis, University of British Columbia, Canada

Evans WH (1941) The strength of undermined strata. Trans Inst Min Metall 50:475–532

Fayol M (1885) Sur les movements de terrain provoques par l'exploitation des mines. Bull Soc Indust Min 14:818

Gere JM, Goodno BJ (2011) Mechanics of materials, 7th edn. Cengage Learning, Stamford, pp 153–162

Hanna K, Conover D, Haramy K (1991) Coal mine entry intersection behavior study. US Bureau of Mines, Washington DC

Hu WY, Yin SX (2010) Dynamic mechanism of water inrush from floor of mining face. Chin J Rock Mech Eng 29(S-1):3344–3349

Huang Z, Jiang ZQ, Zhu SY (2014) Characterizing the hydraulic conductivity of rock formations between deep coal and aquifers using injection tests. Int J Rock Mech Min Sci 71:12–18. doi:10.1016/j.ijrmms.2014.06.017

Jin ZM (2006) Theory and technology of top coal caving mining. China Coal Industry Publishing House, Beijing

Kuznetsov ST, Pekarskii DG, Korovkin VT (1973) Determining the normal stresses in a uniform bent beam cantilever. Sov Min Sci 9(5):478–482

Li BY (1999) The "Lower three zones" theory on preventing floor water inrush and its development together with application. J Shandong I Min Technol 4:11–18 **(in Chinese)**

Li BY, Shen GH, Jing ZG, Gao H (1988) The theory and practice of preventing water inrush in mining working face. Saf Coal Min 5:47–48 **(in Chinese)**

Liu HH (2014) Fundamental concept of indication layer in coal floor mining under water pressure. China University of Mining and Technology Press, Xuzhou, pp 59–63

Majumdar S (1986) The support requirement at a longwall face—a bending moment approach. In: Proceedings of 27th US symposium rock mechanics: key to energy production, University of Alabama, Tuscaloosa, AL, USA, pp 325–332

Manteghi H, Shahriar K, Torabi R (2012) Numerical modelling for estimation of first weighting distance in longwall coal mining—a case study. In: Proceedings of 12th coal operators' conference, University of Wollongong and the Australasian Institute of Mining and Metallurgy, pp 60–68

Mojtaba R, Abdolreza YC, Siamak HY (2013) A novel fuzzy inference system for predicting roof fall rate in underground coal mines. Saf Sci 55:26–33. doi:10.1016/j.ssci.2012.11.008

Mueller AR (2010) An analysis of current intersection support and falls in united states coal mines and recommendations to improve safety. MS Thesis, Southern Illinois University Carbondale, USA

Obert L, Duvall WI (1967) Rock mechanics and the design of structures in rock. Wiley, New York

Pawlowicz K (1967) Classification of rock cavability of coal measure strata in Upper Silesia coalfield. Prace GIG, Komunikat, Katowice, No. 429 (in Polish)

Peng SS (2008) Coal mine ground control, 3rd edn. West Virginia University, Department of Mineral Engineering, Morgantown

Peng SS, Chiang HS (1982) Roof stability in longwall coal faces. In: Proceeding of 1st international conference on underground stability, Vancouver, Canada

Peng SS, Chiang HS (1984) Longwall mining. Wiley, New York

Please CP, Mason DP, Hutchinson AJ, Khalique CM, Ngnotchouye JMT, Merwe JNVD, Yilmaz H (2013) Fracturing of an Euler–Bernoulli beam in coal mine pillar extraction. Int J Rock Mech Min Sci 64:132–138. doi:10.1016/j.ijrmms.2013.08.001

Sainoki A, Mitri HS (2014) Dynamic behaviour of mining-induced fault slip. Int J Rock Mech Min Sci 66:19–29. doi:10.1016/j.ijrmms.2013.12.003

Sarkar SK, Chatterjee TK (1992) Single lift extraction of thick seam by longwall mining under Indian geo-mining conditions. In: Proceedings of international symposium on thick seam mining, CMRI, Dhanbad, India, pp 213–224

Sarkar SK, Dhar BB (1993) Strata control failures at caved longwall faces in India—experience from Raffinato Churcha (1964–1990). In: Proceedings of 4th Asian Mining, MGMI, Calcutta, India, pp 361–380

Sarkar SK, Roychoudhary S, Singh B (1988) Recent experiences with mechanised longwall mining with caving in India. In: Proceeding of international symposium on modern mining technology, Shandong Institute of Mining and Technology, China, pp 177–186

Shen GH, Li BY, Wu G (1992) The theory and practice on special mining of mines. China Coal Industry Publication House, Beijing, pp 56–72

Shi YW (1985) Possibility and approaches for developing more compact and light weight powered support. In: Proceedings of international symposium on mining technology and science, China Institute of Mining and Technology, Xuzhou, China, pp 55–66

Shi LQ, Han J (2004) Floor water-inrush mechanism and prediction. China University of Mining and Technology Press, Xuzhou

Singh GSP (2014) Conventional approaches for assessment of caving behavior and support requirement with regard to strata control experiences in longwall workings. J Rock Mech Geotech Eng. doi:10.1016/j.jrmge.2014.08.002

Singh TN, Singh B (1979) Design of support system in caved longwall faces. In: Proceeding of colloquium on longwall face supports, Dhanbad, India, pp 79–85

Singh TN, Singh B (1982) Design criteria of face supports. In: Proceeeding of symposium on state of the art of ground control in longwall mining and mining subsidence, Society of Mining Engineers, New York, USA

Singh GSP, Singh UK (2009) A numerical modeling approach for assessment of progressive caving of strata and performance of hydraulic powered support in longwall workings. Comput Geotech 36(7):1142–1156. doi:10.1016/j.compgeo.2009.05.001

Sterling RL (1980) The ultimate load behaviour of laterally constrained rock beams. In: Proceeding of 21st US symposium on rock mechanics, American Rock Mechanics Association, Rolla, Missouri, USA, pp 33–42

Tahoony SH (2009) Strength of materials. Parsaeen Press, Tehran **(in Persian)**

Timoshenko S, Woinowsky-Krieger S (1959) Theory of plates and shells. McGraw-Hill, New York

Tsesarsky M, Hatzor YH (2003) Deformation and kinematics of vertically jointed rock layers in underground openings. In: Proceedings of 6th International Conference on ICADD-6, Trondheim, Norway, pp 93–102

Unrug KDA, Szwilski ABA (1980) Influence of strata control parameters on longwall mining design. In: Proceedings of 21st US symposium on rock mechanics, American Rock Mechanics Association, Rolla, Morgantown, WV, USA

Wang ZY, Liu HQ, Wang PY, Yu SC (1994) Theory and practice of coal mining discipline on confined water. J China Coal Soc 19(1):40–46 **[in Chinese]**

Wasantha PLP, Ranjith PG (2014) Water-weakening behavior of Hawkesbury sandstone in brittle regime. Eng Geol 178:91–101. doi:10.1016/j.enggeo.2014.05.015

Xiao YC (2013) Mechanism of floor water inrush caused by rock-mass breakage and seepage flowing of confined-water and its engineering practice. Ph.D. Thesis, China University of Mining and Technology, Beijing

Xu ZM (2010) Mining-induced floor failure and the model, precursor and prevention of confined water inrush with high pressure in deep mining. Ph.D. Thesis, China University of Mining and Technology, Beijing

Zhang ZW (2014) Research on rock mass structure characteristics and water inrush risk of the No. 10 coal seam floor at Qingdong mine. Ph.D. Thesis, Anhui University of Science and Technology, Huainan, China

Zhang WQ, Li BY, Li JX, Wang Z (1992) Research on the spatial distribution law of mine water-inrush points. Zhongzhou Coal 1:6–9 **[in Chinese]**

Zhao HZ (1985) A study of strata behavior and support resistance of a fully mechanized longwall face. In: Proceeding of international symposium mining technology and science, China Inst of Mining and Technology, Xuzhou, China, pp 67–73

Zhou ZH, Cao P, Ye ZY, Zhao YL, Wan W (2014) Failure characteristics of pre-stress fractured rock under uniaxial cyclic loading and seepage water pressure. J Min Saf Eng 32(2):293–298 **[in Chinese]**

Zhu SY, Cao DT, Zhou HY, Yang CW, Liu JG (2014) Restrictive function of lithology and its composite structure on deformation and failure depth of mining coal seam floor. J Min Saf Eng 31(1):90–96 **(in Chinese)**